Fe diffusion in amorphous and nanocrystalline alloys studied using nuclear resonance reflectivity

Ajay Gupta,[1] Mukul Gupta,[2] Sujoy Chakravarty,[1] Rudolf Rüffer,[3] Hans-Christian Wille,[3] and Olaf Leupold[3]
[1]*Inter-University Consortium for DAEF, University Campus, Khandwa Road, Indore 452017, India*
[2]*Laboratory for Neutron Scattering, ETHZ & PSI, CH-5232 Villigen PSI, Switzerland*
[3]*European Synchrotron Radiation Facility, Boîte Postale 220, F-38043 Grenoble Cedex, France*
(Received 6 January 2005; revised manuscript received 31 March 2005; published 27 July 2005)

It is demonstrated that nuclear resonance reflectivity from isotopic multilayers can be used as a sensitive technique to study self-diffusion of a Mössbauer isotope (^{57}Fe in the present case). In the case of isotopic multilayers, in which alternate layers have the same chemical composition and differ only in the abundance of ^{57}Fe, nuclear resonance scattering causes x-ray scattering contrast between adjacent layers, resulting in the appearance of Bragg peaks corresponding to the bilayer periodicity. Diffusion of ^{57}Fe across the isotopic interface results in a decrease in the scattering contrast and thus a decrease in the intensity of the Bragg peak, making it possible to measure diffusion lengths of the order of 0.1 nm in *chemically homogeneous* films. The technique has been used to study self-diffusion of Fe in amorphous FeZr and nanocrystalline FeN alloys. In a-FeZr, measurements yield activation energy for Fe diffusion $E=0.42\pm0.05$ eV and the pre-exponent factor $D_0=\exp(-39\pm1)$ m^2/s. In nanocrystalline $Fe_{60}N_{40}$, variation in diffusivity due to structural relaxation at temperatures as low as 393 K could be observed. Measurements in the structurally relaxed state yield $E=0.8\pm0.2$ eV and $D_0=\exp(-28\pm4)$ m^2/s.

DOI: 10.1103/PhysRevB.72.014207 PACS number(s): 76.80.+y, 66.30.Fq

I. INTRODUCTION

Mössbauer spectroscopy is a well-established technique for studying atomic diffusion in solids.[1–5] Conventionally, diffusion measurements have been done by studying the effects of diffusive motion on the shape of the resonance lines.[1,2] More recently, a much more powerful method of nuclear resonance forward scattering of synchrotron radiation has been used which relies on the time domain measurement of the scattered intensity, and the information about the diffusive motion is obtained through the modulation of the time dependence of the intensity of the resonantly scattered radiation.[3–5] In both the frequency domain as well as time domain measurements, the intensity distribution of the Mössbauer radiation gets modified significantly only when the time scale of the diffusive motion is comparable to the lifetime of the nuclear excited state participating in the resonance scattering. This puts limits on the range of diffusivity that can be measured using this technique. In the case of ^{57}Fe Mössbauer resonance, typical diffusivities that can be measured lie in the range 10^{-12} to 10^{-13} m^2/s. In the present work we demonstrate the possibility of using nuclear resonance scattering from isotopic multilayers for studying self-diffusion of Mössbauer isotopes over a range several orders of magnitude larger than that accessible through the above techniques. At the same time, the technique is sensitive enough to measure diffusion lengths as small as 0.1 nm, which is more than an order of magnitude larger than the sensitivity of conventional depth-profiling techniques such as secondary ion mass spectroscopy (SIMS), and auger electron spectrometry (AES).[6,7]

Atomic diffusion in amorphous and nanocrystalline alloys has been a subject of great interest, as changes in the structure of these alloys and their relation to physical properties are of primary interest from the points of view of their technological applications and stability against external environment.[6–12] Several experimental techniques have been used to study self-diffusion of the constituent species in amorphous and nanocrystalline alloys.[8] Depth profiling using radioactive tracer or SIMS have been the most extensively used techniques for such studies. However, typical depth resolution of these techniques is a few nm, and this limits the minimum diffusion length which can be measured. It may be noted that the thermal stability of amorphous and nanocrystalline alloys is generally not very high and, therefore, diffusion annealing has to be done at relatively low temperatures (typically 400 K–700 K). As a result, the diffusion lengths achievable within a reasonable annealing time can be as small as a nanometer. Also, both amorphous and nanocrystalline alloys exhibit structural relaxation at still lower temperatures and a possible study of the effects of structural relaxation on atomic diffusivity would involve measurement of diffusion lengths of the order of 0.1 nm. Therefore, there is a strong need to use experimental techniques with a possibility to measure diffusion lengths smaller than a nanometer. X-ray reflectivity from compositionally graded multilayers is one such technique which has been used to measure diffusion lengths as small as 0.1 nm.[11] However, such measurements yield interdiffusion coefficients which pertain to diffusion in a chemically inhomogeneous material. In contrast, nuclear resonance reflectivity from isotopic multilayers, proposed in the present work, can be used to study self-diffusion in chemically homogeneous systems: the alternate layers have the same chemical compositions and differ only in the isotopic abundance of the Mössbauer atom, e.g., ^{57}Fe. Therefore, there is no contrast between the adjacent layers as far as the x-ray scattering from the electron density in the material is concerned. However, if the energy of the incident radiation is tuned to the nuclear resonance energy of ^{57}Fe, large scattering contrast develops between layers containing natural Fe and ^{57}Fe due to strong nuclear resonance scatter-

ing from ^{57}Fe nuclei. This results in a Bragg peak in the reflectivity corresponding to the bilayer periodicity of the multilayer.[13–15] Height of this Bragg peak can be monitored to get information about the interdiffusion of the ^{57}Fe isotope across the interfaces.

In the present work, we have used nuclear resonance reflectivity to study self-diffusion of Fe in two systems, namely, amorphous FeZr alloy and nanocrystalline FeNZr. The two systems have been chosen for the following reasons: Amorphous alloys of late transition metal and early transition metals have been extensively studied for self-diffusion measurements, and extensive data on self-diffusion in this class of alloys is available in the literature.[6,8] Therefore, the results of measurements on FeZr amorphous alloy can be compared with the results in the literature. The other system is nanocrystalline nitride. Self-diffusion of Fe in amorphous $FeN_{0.7}$ alloy has already been studied, and it is found that the diffusion mechanics is similar to that in other transition metal metalloid metallic glasses.[7] It would be interesting to compare the self-diffusion of Fe in a nanocrystalline alloy of similar composition with that in amorphous alloy. A small amount of Zr was added to this system in order to restrict the grain size so as to produce nanocrystalline structure; it is well known that addition of a small amount of early transition metal in transition metal metalloid systems results in inhibition of grain growth and formation of a nanocrystalline phase.[16]

II. THEORETICAL CONSIDERATIONS

In the presence of nuclear resonance scattering, the total scattering amplitude of an atom can be written as a sum of the scattering amplitude due to electronic scattering and that due to nuclear resonance scattering. As a result, at grazing incidence geometry, the index of refraction of the layer material can be written as

$$n_{ab} = \sqrt{1 + \frac{\lambda_0^2}{\pi}\sum_i \sigma_i (f_i)_{ab}} \approx 1 + \frac{\lambda_0^2}{2\pi}\sum_i \sigma_i [(f_i^e)_{ab} + (f_i^n)_{ab}], \tag{1}$$

where $(f_i^e)_{ab}$ and $(f_i^n)_{ab}$ are the electronic and nuclear scattering amplitudes for scattering $\vec{\mathcal{E}}_b$-polarized radiation into $\vec{\mathcal{E}}_a$-polarized radiation, respectively, and σ_i is the atomic density of the species i. For forward scattering, away from the absorption edge, for an isotropic dipole oscillator and no polarization mixing, the electronic scattering amplitude is given by

$$(f^e)_{ab} = \delta_{ab} f^e = -Zr_e + \frac{i\sigma_e}{4\pi\bar{\lambda}_0}, \tag{2}$$

where $r_e = e^2/mc^2$ is the classical radius of electron and σ_e is the photoelectric cross-section. Thus, the electronic contribution to the refractive index has only a weak dependence on the x-ray energy. On the other hand, for the present case of Mössbauer transition of ^{57}Fe nuclei (M1 transition), in absence of a magnetic splitting, and a polycrystalline sample, the nuclear scattering amplitude can be written as[17]

$$(f^n)_{ab} = \delta_{ab}\frac{\lambda_0}{4\pi}\frac{f_{LM}}{1+\alpha}\frac{2j_1+1}{2j_0+1}\frac{A}{x-i}, \tag{3}$$

where $x = (\Delta E - \hbar\omega)/\Gamma_0$, A denotes for inhomogeneous broadening, ΔE is the quadrupole splitting, Γ_0 the natural line width, and f_{LM} is the Lamb-Mössbauer fraction. The nuclear scattering amplitude exhibits a strong energy dependence around the resonance, and in this energy region it dominates over the electronic scattering amplitude. Since the chemical composition of the alternate layers is identical, there is no contrast due to the electronic scattering, and the only contrast comes due to the different concentration of ^{57}Fe nuclei in them.

The reflectivity of the multilayer can be calculated using Parratt's formalism, by coherently summing the reflected amplitudes over the energy width of the incident radiation.[18] However, for the present purpose, the diffusion lengths L_d can be obtained without taking recourse to a detailed fitting of the reflectivity pattern in the following manner: depth dependence of the abundance of ^{57}Fe isotope in the isotopic multilayer can be expressed as a Fourier series[12]

$$C(z) = \sum_n C_n \exp(ik_n z), \tag{4}$$

with $k_n = 2n\pi/\lambda$, and λ being the periodicity of the multilayer. When a multilayer is annealed and its constituents interdiffuse, the amplitudes C_n decay with time. According to the one-dimensional diffusion equation, it can be written as

$$C_n = C_{0n}\exp[-k_n^2 D(T)t], \tag{5}$$

$D(T)$ being the diffusivity at temperature T. Intensity of the nth Bragg peak in the reflectivity is proportional to square of the amplitude C_n, and thus one can write[12]

$$\ln\left(\frac{I(t)}{I_0}\right) = -\frac{8\pi^2 n^2}{\lambda^2}D(T)t, \tag{6}$$

where I_0 is the intensity of the nth order Bragg peak at $t=0$. The diffusion length in turn is related to the diffusivity $D(T)$ at the annealing temperature T, through the relation $L_d = \sqrt{2D(T)t}$. Therefore, the slope of the annealing time dependence of L_d^2 yields diffusivity at a given temperature. Thus, by monitoring the intensity of the first Bragg peak as a function of the annealing time, one can obtain the diffusivity at a given temperature. The atomic diffusion, which is a thermally activated process, is known to follow the relation $D = D_0\exp(-E/k_BT)$, where E is the activation energy and D_0 is the pre-exponent factor, which contains the details of the diffusion mechanism.[19] The observed temperature dependence of diffusivity has been used to obtain E and D_0 for Fe self-diffusion in the alloys, which in turn provide some insight into the diffusion mechanism.

III. EXPERIMENTAL DETAILS

Thin films of amorphous FeZr alloy were made by ion beam sputtering of a composite target of Fe and Zr with an Ar (purity 99.9995%) ion beam of 800 eV energy and a

beam current of 25 mA.[20] The ion gun used was a 3 cm broad-beam Kaufman-type hot-cathod gun (Commonwealth Scientific Corporation). With a base vacuum of 1×10^{-7} mbar, the Ar gas flow in the chamber was controlled using a mass flow controller (MKS-MFC 1179A) at 6.0 cm^3/min. Initially the chamber was flushed repeatedly with argon gas to remove contamination of other gases. The ion beam was incident at the target at an angle of 45° from the line of beam and the substrates were kept at a distance of about 20 cm in a direction parallel to the target. Small pieces of zirconium were fixed on the iron target and both the targets were co sputtered. The area covered by the Zr target was controlled in order to achieve the desired composition of the deposited alloy. For preparing isotopic multilayers, two different targets, one with normal Fe and the other one with 95% enriched ^{57}Fe, were used. The nominal structure of the multilayer was float glass substrate/$Fe_{70}Zr_{30}$ 4 nm/[$^{57}Fe_{70}Zr_{30}$ 3 nm/$Fe_{70}Zr_{30}$ 4 nm] $\times 10$.

Nanocrystalline FeNZr was prepared by magnetron sputtering of composite FeZr targets. A mixture of nitrogen and argon gases (50% each) was used to sputter the composite target with a power of 50 W. Small amounts of Zr in this case were essentially used in order to restrict the grain size of FeN. The nominal structure of the multilayer in this case was float glass substrate/[FeNZr 4 nm/^{57}FeNZr 3 nm]$\times 20$. Samples were annealed in an atmosphere of flowing nitrogen. The temperature of the furnace was controlled with an accuracy of ±1 K. Samples were inserted in a pre heated furnace in order to minimize the time to reach the stipulated temperature.

Nuclear reflectivity of the multilayer was measured at the beamline ID22N of European Synchrotron Radiation Facility, Grenoble.[21] The storage ring operated in 16-bunch mode providing short pulses of x rays every 176 ns. The radiation from the undulator source, optimized for the 14.4 keV transition in iron, was filtered by a double Si(111) reflection followed by a high-resolution nested monochromator.[21] The delayed events, resulting from the nuclear forward scattering, were counted by a fast avalanche photodiode (APD) detector. While the prompt events gave the usual electronic reflectivity, delayed events were used to obtain the nuclear resonance reflectivity.

IV. RESULTS AND DISCUSSION

Amorphous FeZr alloy

As prepared, the FeZr alloy multilayer film was characterized using x-ray diffraction (XRD), conversion electron Mössbauer spectroscopy (CEMS), and x-ray photoelectron spectroscopy (XPS). XPS measurements gave the composition of the film as $Fe_{70}Zr_{30}$. Absence of any crystalline peak in the XRD pattern of the as-deposited film confirms its amorphous nature. CEMS of the film consists of a broad singlet as shown in Fig. 1(a). The spectrum has been fitted with a distribution of quadrupole splitting, which reflects the distribution of the local environment due to the amorphous nature of the film. The average isomer shift and quadrupole splitting come out to be -0.09 ± 0.01 mm/s and 0.55 ± 0.01 mm/s respectively. Figure 1 gives the CEMS of the specimen after isochronal annealing at different temperatures. It may be noted that up to 673 K there is only small variation in the hyperfine field parameters, which may be associated with some structural relaxation in the amorphous structure. Annealing at 723 K results in appearance of an additional magnetic component corresponding to the α-Fe phase. Thus, Mössbauer measurements suggest that the amorphous phase is stable up to 673 K. Beyond this temperature it crystallizes, with α-Fe being the primary crystalline phase. Figure 2 shows the x-ray reflectivity pattern of the isotopic multilayer. The reflectivity pattern exhibits only the Kiessig oscillations due to the total thickness of the film. Absence of any Bragg peak corresponding to the bilayer periodicity suggests that the chemical composition of the two isotopic layers is similar and thus they differ only in the isotopic abundance of Fe. A detailed fitting of the reflectivity curve using Parratt's formalism[18] gives the total thickness of

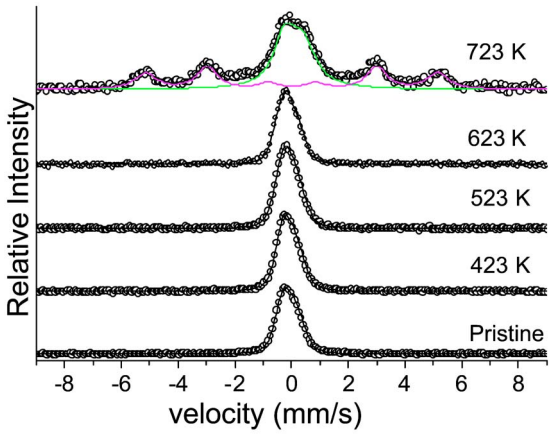

FIG. 1. (Color online) Conversion electron Mössbauer spectra of the amorphous $Fe_{70}Zr_{30}$ film as a function of isochronal annealing at different temperatures. Continuous curves represent fit to the experimental data.

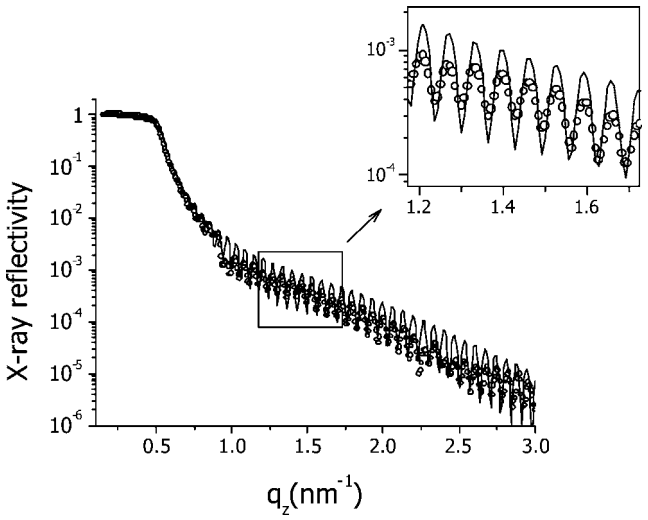

FIG. 2. X-ray reflectivity of the $^{57}Fr_{70}Zr_{30}/Fe_{70}Zr_{30}$ multilayer taken using Cu $K\alpha$ radiation.

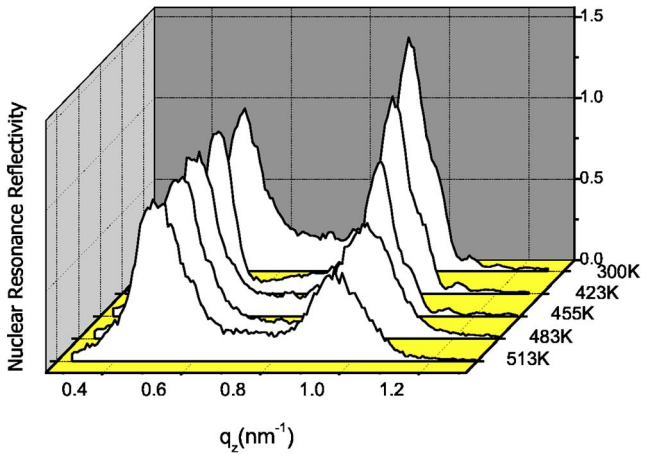

FIG. 3. (Color online) Nuclear resonance reflectivity of the $^{57}Fr_{70}Zr_{30}/Fe_{70}Zr_{30}$ multilayer taken at the Mössbauer resonance energy of ^{57}Fe (14.413 keV), as a function of isochronal annealing at different temperatures. The Bragg peak around $q=0.9$ nm^{-1} corresponds to the isotopic periodicity of the multilayer.

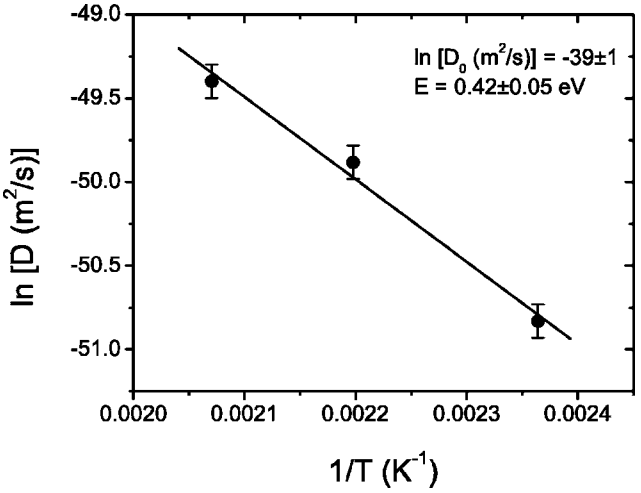

FIG. 4. Arrhenius behavior of diffusion coefficient with isochronal annealing temperature for a FeZr multilayer.

the film as 90.0 nm and the roughness of the glass-to-film and film-to-air interfaces as 0.5 nm and 0.5 nm respectively. Therefore, the actual structure of the multilayer is substrate/$Fe_{70}Zr_{30}$ 4.87 nm/[$^{57}Fe_{70}Zr_{30}$ 3.65 nm/$Fe_{70}Zr_{30}$ 4.87 nm]$\times 10$.

Figure 3 gives the nuclear resonance reflectivity of the as-deposited multilayer as well as after isochronal annealing at various temperatures for 30 min each, in the q range 0.2 to 1.2 nm^{-1}. Acquisition of each reflectivity pattern took a time of only about 30–45 min. In addition to the peak at the critical angle ($q_c \sim 0.5$ nm^{-1}), a strong first-order Bragg peak due to multilayer periodicity can be clearly seen around $q=0.9$ nm^{-1}. Further, one can clearly see that the height of the Bragg peak goes down with thermal annealing as a result of the diffusion of Fe across the isotopic interfaces. The intensity of the Bragg peak was obtained by first removing the q^{-4} dependence of the Fresnel reflectivity,[18] and then taking the area under the peak. The temperature-dependent intensity of the Bragg peak is used to get the diffusion coefficient at each temperature using Eq. (6). The values of diffusion coefficient obtained at different temperatures are used to calculate activation energy E and pre-exponential factor D_0 using the equation $D=D_0 \exp(-E/K_BT)$, where T is the annealing temperature (Fig. 4). The activation energy for self-diffusion of Fe in the present system comes out to be 0.42 ± 0.05 eV and pre-exponential factor $D_0=\exp(-39\pm1)$ m^2/s. This value is substantially lower as compared to that in FeZr metallic glasses of similar composition.[8,9,22] This low activation energy can be attributed to the fact that the present results pertain to amorphous film which would have a higher density of defects, and that the measurements have been done in the unrelaxed state of the system.

Nanocrystalline FeNZr alloy

Figure 5 shows the x-ray photoelectron spectra of the FeNZr multilayer sample. The binding energy of the Fe $2p_{3/2}$ core level corresponds to that of FeN while the Zr $3d_{5/2}$ level shows two peaks corresponding to metallic Zr and ZrO_2. The stoichiometry of the film as obtained from the XPS data is $Fe_{64}N_{26}Zr_{10}$. A small amount of oxygen was also detected.

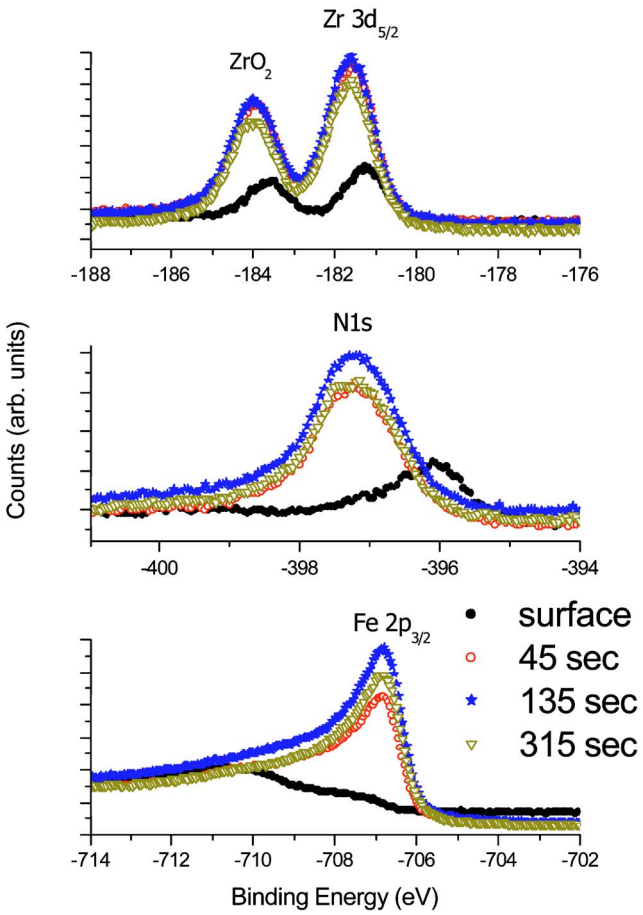

FIG. 5. (Color online) XPS spectra of FeNZr film covering the binding energy ranges corresponding to Zr $3d_{5/2}$, N $1s$, and Fe $2p_{3/2}$ levels.

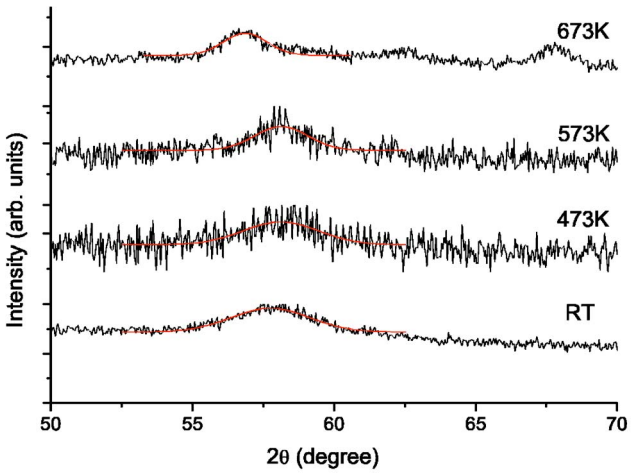

FIG. 6. (Color online) XRD pattern of nanocrystalline FeNZr film as a function of isochronal annealing at different temperatures. The solid curves represent Gaussian fit to the line profile, which has been used to estimate the crystallite size.

Figure 6 gives the x-ray diffraction pattern of the $Fe_{64}N_{26}Zr_{10}$ film after annealing at different temperatures for a period of 30 min each. The diffraction pattern of the as-deposited film exhibits broad peaks at a scattering angle corresponding to the γ-iron nitride phase. The crystallite size as obtained from the width of the diffraction peaks is given in Table I. Thermal annealing up to 573 K shows only a small variation in the XRD pattern; however, annealing beyond 573 K results in appearance of additional peaks, suggesting that the obtained phase is metastable and transforms to other phases above 573 K. From Table I it can further be seen that annealing up to 473 K does not cause any change in the grain size. However, annealing at 573 K results in some grain growth.

Figure 7 gives the Mössbauer spectrum of the pristine sample as well as the samples annealed at different temperatures. In all cases, the spectrum consists of a broad doublet. The Mössbauer spectrum of the pristine sample has been analyzed in accordance with the results in the literature on nonmagnetic iron nitride, with two doublets and two singlets.[23] The results of the fitting of the Mössbauer spectra are given in Table I. The fitted parameters are very close to those of crystalline $Fe_{0.6}N_{0.4}$.[23] It may be noted that the Mössbauer spectrum of amorphous $Fe_{0.6}N_{0.4}$ is also qualitatively similar to that of crystalline $Fe_{0.6}N_{0.4}$.[7] However, as expected, the Mössbauer parameter of the present sample are closer to those of crystalline $Fe_{0.6}N_{0.4}$ as compared to those of amorphous compound. These results also suggest that Zr does not go inside the FeN nanocrystals. This is again as per expectation, since in case of finemet and nanoperm alloys it is known that the early transition metal element (Nb, Zr, Ta) that is added for inhibiting the grain growth is not retained

TABLE I. Results of computer fitting of the XRD and Mössbauer spectra of nanocrystalline FeNZr film as a function of isochronal annealing at different temperatures. In accordance with the results in the literature (Ref. 21), Mössbauer spectra have been fitted with two doublets and two singlets. In the XRD pattern, peak around $2\theta=48°$ has been fitted with a Lorentzian in order to obtain the lattice spacing d and the grain size.

Ann. Temp. (K)	Sub-spectrum	Isomer-shift (mm/s)	Quadrupole splitting (mm/s)	Area (%)	d value (nm)	Grain Size (nm)
300	Singlet 1	0.53±0.01	—	14	0.159±0.007	0.6±0.1
	Singlet 2	0.06	—	27		
	Doublet 1	0.63	0.72±0.01	14		
	Doublet 2	0.29	0.85	45		
373	Singlet 1	0.53	—	14	0.158	2.5±0.2
	Singlet 2	0.06	—	30		
	Doublet 1	0.63	0.72	16		
	Doublet 2	0.29	0.85	40		
473	Singlet 1	0.53	—	17	0.158	2.8±0.2
	Singlet 2	0.06	—	30		
	Doublet 1	0.64	0.72	17		
	Doublet 2	0.29	0.85	36		
573	Singlet 1	0.53	—	07	0.158	4.8±1
	Singlet 2	0.07	—	50		
	Doublet 1	0.59	0.75	13		
	Doublet 2	0.28	0.86	30		
673	Singlet 1	0.54	—	16	0.162	5.6±1
	Singlet 2	0.25	—	30		
	Doublet 1	0.61	0.58	36		
	Doublet 2	0.31	0.74	18		

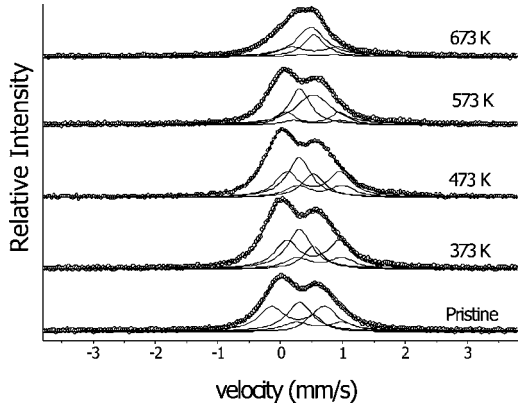

FIG. 7. Conversion electron Mössbauer spectra of nanocrystalline FeNZr film as a function of isochronal annealing at different temperatures. Continuous curves represent fit to the experimental data.

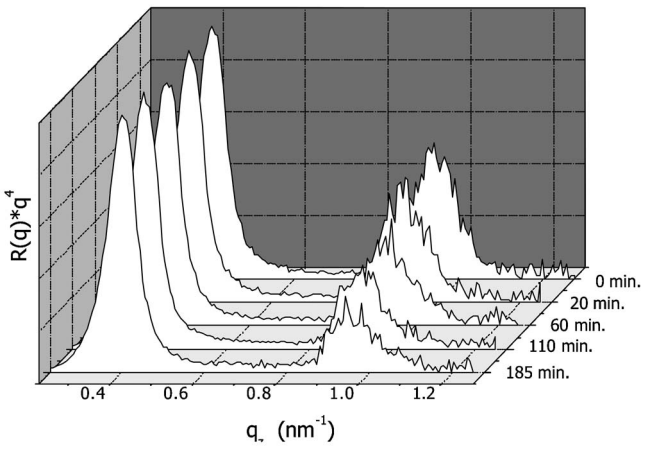

FIG. 8. Nuclear resonance reflectivity of the ^{57}FeNZr/FeNZr multilayer taken at the Mössbauer resonance energy of ^{57}Fe (14.413 keV), as a function of annealing time at 393 K.

inside the nanocrystals; rather it goes to the grain-boundary region.[16] Thus, Mössbauer, XRD, and XPS measurements suggest that the structure of FeNZr film consists of nanograins of γ-iron nitride, while Zr goes to the grain-boundary region. The stoichometry of the nanograins is $Fe_{1-x}N_x$, with $0.3 < x < 0.4$. From the x-ray reflectivity the total thickness of the FeNZr isotopic multilayer comes out to be 139 nm. Accordingly, the structure of the multilayer is substrate/[FeNZr 3.97 nm/^{57}FeNZr 2.98 nm]$\times$20. Again, absence of any Bragg peak corresponding to the isotopic periodicity suggests that the multilayer is chemically homogeneous.

Perusal of Table I shows that annealing up to 573 K does not result in any significant change in the hyperfine field parameters, indicating that the local environment of Fe remains unchanged up to 573 K. Annealing up to 673 K results in a qualitative change in the shape of the Mössbauer spectrum and hyperfine field parameters. Thus Mössbauer measurements show that, as prepared, the nanocrystalline phase is stable only up to 573 K. Therefore, for diffusion measurements, it is necessary that the annealings are done at temperatures below 473 K so as to avoid any microstructural changes during diffusion annealings. Since the diffusion lengths obtainable within reasonable annealing times at such low temperatures are expected to be small, a sensitive technique such as nuclear resonance scattering is necessary for studying atomic diffusion in the system. Isothermal annealing was done at three different temperatures, namely, 393 K, 423 K, and 448 K.

Figure 8 gives the nuclear resonance reflectivity pattern of the multilayer after isothermal annealing at 393 K for different periods of time. Self-diffusion of Fe across the isotopic interface results in a decrease in the contrast for nuclear resonance scattering between the adjacent layers resulting in a gradual decrease in the reflectivity at the first Bragg peak. As in the case of amorphous FeZr multilayer, the intensity of the Bragg peak was obtained by first removing the q^{-4} dependence of the Fresnel reflectivity,[18] and then taking the area under the peak. Figure 9 gives the annealing time dependence of the square of the diffusion length at the three different temperatures. It may be noted that, in general, a detailed fitting of reflectivity data acquired over a sufficiently large q-range (covering several orders of multilayer Bragg peaks) can yield the roughness/interdiffusion at the interfaces with an accuracy of 0.05 nm.[24] However, in the present case, since the diffusion length is determined from the intensity of the first Bragg peak only, the accuracy is rather limited. From Fig. 9 it can be seen that for all three annealing temperatures, the diffusion length initially increases at a faster rate and that after a certain annealing time the rate becomes constant. The initial faster increase in the diffusion length may be associated with the structural relaxation in the system. Studies have

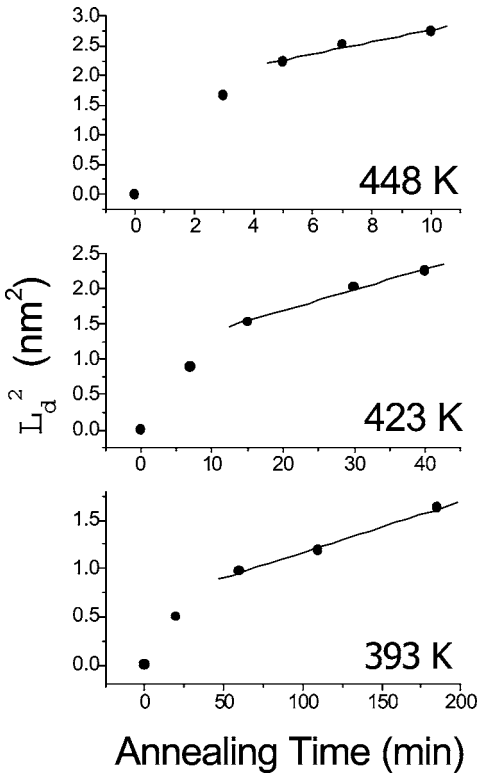

FIG. 9. Annealing time dependence of the diffusion length in a FeNZr film at various temperatures.

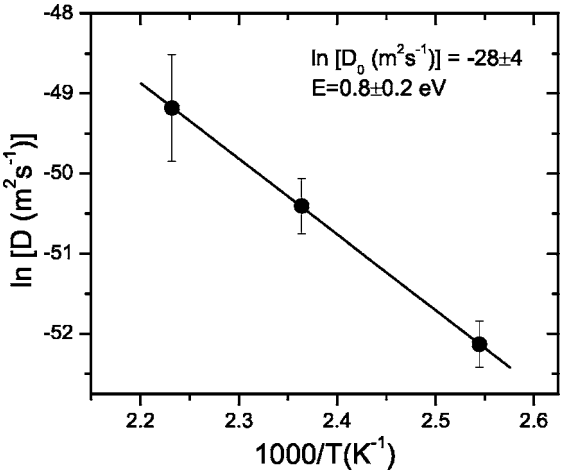

FIG. 10. Arrhenius behavior of diffusion coefficient with isothermal annealing temperature for FeNZr multilayer.

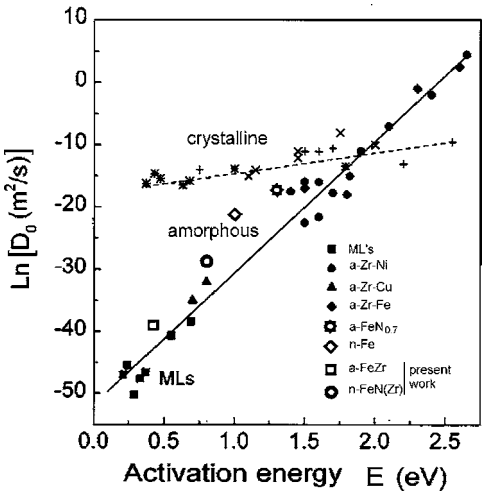

FIG. 11. Plot of $\ln D_0$ vs E for various amorphous and crystalline alloys showing correlation between the two quantitites. Amorphous and crystalline systems exhibit distinctly different $\ln D_0 - E$ correlations. Data has been taken from Refs. 23, 25, and 7. For comparision, data for a-$Fe_{70}Zr_{30}$ and n-FeNZr as obtained in the present work have also been plotted.

shown that nanocrystalline alloys also exhibit structural relaxation similar to amorphous alloys. This relaxation is associated with the relaxation of the highly disordered grain-boundary region, stress relaxation in the film, and annealing out of the defects inside the nanocrystals.[25] From Table I it may be seen that annealing at 473 K results in a small decrease in the lattice parameter of the nanocrystalline phase, which again is an indication of the structural relaxation in the system. Slope of the curve in Fig. 9 for longer annealing times was used to calculate the diffusivity at different temperatures in the structurally relaxed state. Figure 10 gives the plot of $\ln(D)$ vs $1/T$. The data are fitted with a straight line yielding the activation energy $E=0.8\pm0.2$ eV and the pre-exponent factor $D_0=\exp(-28\pm4)$ m^2/s. It may be noted that the activation energy for self-diffusion of Fe in the present system is significantly lower than that in the amorphous FeN of similar composition.[7] This result is in general agreement with the earlier studies where the low activation energy for diffusion in nanocrystalline alloys has been attributed to a higher density of grain boundaries.

The pre-exponent factor D_0 in amorphous alloys exhibit a variation over a much wider range as compared to that in crystalline alloys, which essentially reflects different mechanisms of diffusion in the two cases.[19] For the same value of the activation energy, D_0 in amorphous alloys can be orders of magnitude different than that in crystalline alloys. This difference in D_0 in the two types of systems is due to the difference in their entropy for diffusion ΔS, which is related to D_0 through relation

$$D_0 = A \exp(\Delta S/k_B). \tag{7}$$

A much larger value of ΔS in amorphous alloys is interpreted as an indication of the coordinated motion of a group of several atoms.[8] Thus, while in crystalline alloys the atomic diffusion is via vacancies or interstitials, in amorphous alloys it involves a collective motion of a large group of atoms. This difference in the diffusion mechanism is also reflected in the difference in the correlation between D_0 and E in the two systems. It has been observed in the literature that the pre-exponential factor D_0 and activation energy E exhibit a correlation of the form[8,26,27]

$$D_0 = A \exp(E/B), \tag{8}$$

where A and B are constants. The above relationship holds for both crystalline and amorphous alloys; however, the values of A and B are very different in two cases, being ($A=10^{-19}$ m^2/s^{-1}, $B=0.055$ eV) and ($A=10^{-7}$ m^{2}s^{-1}, $B=0.41$ eV), for amorphous and crystalline alloys respectively.[8] Figure 11 presents the $\ln D_0$ vs E data for both crystalline as well as amorphous alloys as taken from the literature.[7,26,28] For comparison, the values obtained for a-$Fe_{70}Zr_{30}$ as well as nanocrystalline FeNZr in the present work are also plotted in Fig. 11. As expected, the point for a-$Fe_{70}Zr_{30}$ lies along the correlation line for the amorphous alloys.

It is interesting to note that the point corresponding to nanocrystalline FeNZr also lies closer to the correlation line for the amorphous phase rather than to that of crystalline phase. It may be pointed out that in nanocrystalline alloys a large-volume fraction is occupied by grain-boundary region and the atomic diffusion is governed predominantly by diffusion through these grain boundaries. The fact that the point for nanocrystalline FeNZr lies closer to the correlation line for the amorphous phase suggests that the structure of the grain-boundary region in this system is closer to that of the amorphous alloys.

It may be noted that the high sensitivity of the present technique enables one to clearly see the initial variation in the diffusivity because of the structural relaxation in the system even at temperatures as low as 393 K, although the typical diffusion lengths involved are of the order of 0.1 nm.

V. CONCLUSIONS

In conclusion, nuclear resonance reflectivity from isotopic multilayers has been used as a sensitive technique to study self-diffusion of a Mössbauer isotope (^{57}Fe). The technique is sensitive enough to measure diffusion lengths as small as a fraction of a nanometer. Self-diffusion of iron in amorphous $Fe_{70}Zr_{30}$ and nanocrystaline $Fe_{60}N_{40}$ has been studied. In both cases, the metastable nature of the systems requires that the diffusion annealings be done at relatively low temperatures and, therefore, a sensitive technique like nuclear resonance reflectivity is essential to measure the small diffusion lengths achievable during reasonable annealing times. In nanocrystalline $Fe_{60}N_{40}$, variation in diffusivity due to structural relaxation at temperatures as low as 393 K could be observed. Activation energy for self-diffusion of Fe in nanocrystalline FeN alloy is found to be smaller than that in amorphous FeN alloy. This result is in general agreement with the earlier studies where a low activation energy for diffusion in nanocrystalline alloys has been attributed to a higher density of grain boundaries. Further, the observed values of D_0 and E suggest that the mechanism of diffusion in this system is similar to that in amorphous alloys.

ACKNOWLEDGMENTS

Thanks are due to Satish Potdar and M. Horisberger for help in depositing isotopic multilayer of FeZr and FeNZr respectively, and to Dr. Fabio Raimondi for help in doing XPS measurements.

[1] K. Ruebenbauer, J. G. Mullen, G. U. Nienhaus, and G. Schupp, Phys. Rev. B **49**, 15607 (1994); R. C. Knauer, J. G. Mullen, Phys. Rev. **174**, 711 (1968).

[2] G. Vogl, in *Mössbauer Spectroscopy Applied to Magnetism and Materials Science*, edited by Gary J. Long and Fernande Grandjean (Plenum Press, New York, 1996), Vol. 2.

[3] B. Sepiol, A. Meyer, G. Vogl, R. Rüffer, A. I. Chumakov, and A. Q. R. Baron, Phys. Rev. Lett. **76**, 3220 (1996).

[4] B. Sepiol, A. Meyer, G. Vogl, H. Franz, and R. Rüffer, Phys. Rev. B **57**, 10433 (1998).

[5] M. Sladecek, B. Sepiol, M. Kaisermayr, J. Korecki, B. Handke, H. Thiess, O. Leupold, R. Rüffer, and G. Vogl, Surf. Sci. **507**, 124 (2002).

[6] A. Grandjean, P. Blanchard, and Y. Limoge, Phys. Rev. Lett. **78**, 697 (1997).

[7] M. Gupta, A. Gupta, S. Rajagopalan, and A. K. Tyagi, Phys. Rev. B **65**, 214204 (2002).

[8] F. Faupel, W. Frank, M.-P. Macht, H. Mehrer, V. Naundorf, K. Rätzke, H. R. Schober, S. K. Sharma, and H. Teichler, Rev. Mod. Phys. **75**, 237 (2003).

[9] A. Heesemann, V. Zöllmer, K. Rätzke, and F. Faupel, Phys. Rev. Lett. **84**, 1467 (2000).

[10] H. Tanimoto, P. Farber, R. Würschum, R. Z. Valiev, and H.-E. Schaefer, Nanostruct. Mater. **12**, 681 (1999); H. Tanimoto, L. Pasquini, R. Prümmer, H. Kronmüller, and H.-E. Schaefer, Scr. Mater. **42**, 961 (2000).

[11] A. L. Greer, Defect Diffus. Forum **143–147**, 557 (1997); Wei-Hua Wang, Hai Yang Bai, Ming Zhang, J. H. Zhao, X. Y. Zhang, and W. K. Wang, Phys. Rev. B **59**, 10811 (1999).

[12] T. Mizoguchi, S. Tanabe, and M. Murata, J. Magn. Magn. Mater. **126**, 96 (1993); A. L. Greer and F. Spaepen, in *Synthetic Modulated Structures* edited by L. L. Chang and B. C. Giessen (Academic Press, Orlando, 1985), p. 419.

[13] A. I. Chumakov, G. V. Smirnov, A. Q. R. Baron, J. Arthur, D. E. Brown, S. L. Ruby, G. S. Brown, and N. N. Salashchenko, Phys. Rev. Lett. **71**, 2489 (1993); R. Röhlsberger, E. Witthoff, E. Gerdau, and E. Lken, J. Appl. Phys. **74**, 1933 (1993).

[14] L. Deák, G. Bayreuther, L. Bottyán, E. Gerdau, J. Korecki, E. I. Kornilov, H. J. Lauter, O. Leupold, D. L. Nagy, A. V. Petrenko, V. V. Pasyuk-Lauter, H. Reuther, E. Richter, R. Röhlsberger, and E. Szilagyi, J. Appl. Phys. **85**, 1 (1999).

[15] Ajay Gupta, Mukul Gupta, B. A. Dasannacharya, Y. Yoda, S. Kikuta, and M. Seto, J. Phys. Soc. Jpn. **73**, 423 (2004).

[16] M. E. McHenry, M. A. Willard, and D. E. Laughlin, Prog. Mater. Sci. **44**, 291 (1999).

[17] J. P. Hannon, N. V. Hung, G. T. Trammell, E. Gerdau, M. Mueller, R. Rüffer, and H. Winkler, Phys. Rev. B **32**, 6363 (1985).

[18] L. G. Parratt, Phys. Rev. **95**, 359 (1954).

[19] V. Naundorf, M.-P. Macht, A. S. Bakai, and N. Lazarev, J. Non-Cryst. Solids **250–252**, 679 (1999).

[20] M. Gupta, A. Gupta, S. M. Chaudhari, D. M. Phase, and B. A. Dasannacharya, Appl. Surf. Sci. **205**, 309 (2003).

[21] R. Rüffer and A. I. Chumakov, Hyperfine Interact. **97/98**, 589 (1996). See also http://www.esrf.fr/exp_facilities/ID18/

[22] J. Horváth, J. Ott, K. Pfahler, and W. Ulfert, Mater. Sci. Eng. **97**, 409 (1988).

[23] L. Rissanen, M. Neubauer, K. P. Lieb, and P. Schaaf, J. Alloys Compd. **274**, 74 (1998).

[24] See for example, M. Tolan, *X-ray Scattering from Soft-Matter Thin Films* (Springer, Berlin, 1999).

[25] H. Tanimoto, L. Pasquini, R. Prummer, H. Kronmuller, and H.-E. Schaefer, Scr. Mater. **42**, 961 (2000); E. Bonetti, E. G. Campari, L. Del Bianco, L. Pasquini, and E. Sampaolesi, Nanostruct. Mater. **11**, 709 (1999).

[26] Wei-Hua Wang, Hai Yang Bai, Ming Zhang, J. H. Zhao, X. Y. Zhang, and W. K. Wang, Phys. Rev. B **59**, 10811 (1999).

[27] W. Linert, Chem. Soc. Rev. **18**, 477 (1989).

[28] R. Würschum, T. Michel, P. Scharwaechter, W. Frank, and H.-E. Schaefer, Nanostruct. Mater. **12**, 555 (1999).